REPORT DOCUMENTATION PAGE

1. REPORT DATE (DD-MM-YYYY) 19-12-2006	2. REPORT TYPE Journal Article		3. DATES COVERED (From - To) 19 Sep 06 – 30 Oct 06

4. TITLE AND SUBTITLE

Effects of phonon coupling and free carriers on band-edge emission at room temperature in n-type ZnO crystals

5a. CONTRACT NUMBER
IN-HOUSE

5b. GRANT NUMBER

5c. PROGRAM ELEMENT NUMBER
61102F

6. AUTHOR(S)

*N. C. Giles, *Chunchuan Xu, M. J. Callahan, Buguo Wang, **J. S. Neal, **L. A. Boatner

5d. PROJECT NUMBER
2305

5e. TASK NUMBER
HC

5f. WORK UNIT NUMBER
01

7. PERFORMING ORGANIZATION NAME(S) AND ADDRESS(ES)

Optoelectronic Technology Branch, Sensors Directorate, Hanscom Air Force Base, MA 01731 AFRL/RYHC, ; *West Virginia University, Morgantown, WV 26506; **Center for Radiation Detection Materials and Systems, Oak Ridge National Laboratory, Oak Ridge, TN

8. PERFORMING ORGANIZATION REPORT

9. SPONSORING / MONITORING AGENCY NAME(S) AND ADDRESS(ES)

Electromagnetics Technology Division   Source Code: 437890
Sensors Directorate
Air Force Research Laboratory
80 Scott Drive
Hanscom AFB MA 01731-2909

10. SPONSOR/MONITOR'S ACRONYM(S)
AFRL-RY-HS

11. SPONSOR/MONITOR'S REPORT NUMBER(S)
AFRL-RY-HS-TP-2008-0023

12. DISTRIBUTION / AVAILABILITY STATEMENT
DISTRIBUTION A: APPROVED FOR PUBLIC RELEASE; DISTRIBUTION UNLIMITED

13. SUPPLEMENTARY NOTES

14. ABSTRACT

Room-temperature photoluminescence has been studied in II-type bulk ZnO crystals representing three different growth methods and having free-carrier concentrations (II) ranging from 10^{13} to 10^{18} cm-:1. The near-band-edge emission has both free-exciton and free-exciton-phonon contributions, with the strength of the phonon coupling dependent on sample defect concentrations. Band-gap shrinkage effects are used to explain a decrease in emission energy for the higher n values. Band filling and hand nonparabolicity are predicted to he important for II> 10^{19} cm-·1. At 300 K, in the absence of free carriers. the free-exciton energy is 3.312±0.004 eV.

15. SUBJECT TERMS
ZnO, CVT-grown ZnO crystals, thin film, bulk

16. SECURITY CLASSIFICATION OF:			17.LIMITATION OF ABSTRACT	18.NUMBER OF PAGES	19a. NAME OF RESPONSIBLE PERSON Michael Callahan
a. REPORT Unclassified	**b. ABSTRACT** Unclassified	**c. THIS PAGE** Unclassified	SAR	4	19b. TELEPHONE NUMBER (include area code) N/A

Effects of phonon coupling and free carriers on band-edge emission at room temperature in n-type ZnO crystals

N. C. Giles[a] and Chunchuan Xu
Physics Department, West Virginia University, Morgantown, West Virginia 26506

M. J. Callahan and Buguo Wang[b]
Air Force Research Laboratory, Sensors Directorate, Hanscom Air Force Base, Massachusetts 01731

J. S. Neal
*Center for Radiation Detection Materials and Systems, and Nuclear Science and Technology Division,
Oak Ridge National Laboratory, Oak Ridge, Tennessee 37831*

L. A. Boatner
*Center for Radiation Detection Materials and Systems, and Materials Science and Technology Division,
Oak Ridge National Laboratory, Oak Ridge, Tennessee 37831*

Room-temperature photoluminescence has been studied in n-type bulk ZnO crystals representing three different growth methods and having free-carrier concentrations (n) ranging from 10^{13} to 10^{18} cm^{-3}. The near-band-edge emission has both free-exciton and free-exciton-phonon contributions, with the strength of the phonon coupling dependent on sample defect concentrations. Band-gap shrinkage effects are used to explain a decrease in emission energy for the higher n values. Band filling and band nonparabolicity are predicted to be important for $n > 10^{19}$ cm^{-3}. At 300 K, in the absence of free carriers, the free-exciton energy is 3.312 ± 0.004 eV. © *2006 American Institute of Physics*. [DOI: 10.1063/1.2410225]

ZnO has a polaron band gap of about 3.37 eV at room temperature, a large exciton binding energy (60 meV), and a large LO-phonon energy (72 meV). Thin-film and bulk ZnO crystals are usually n type. The room-temperature electron concentration (n) is about 10^{17} cm^{-3} for crystals grown by the chemical vapor transport (CVT) technique.[1] Hydrothermally grown ZnO is typically less n type due to compensation of donors by Li acceptors.[2] Crystals grown by the high-pressure melt technique can have n values comparable to CVT-grown crystals. Models such as donor-hole (D,h), donor-acceptor, free exciton (FX), and FX-phonon have been invoked to explain near-band-edge 300 K photoluminescence (PL) from ZnO crystals having a wide range of conductivities. Variations in emission energies of many tens of meV are observed for samples grown by different techniques and with different doping concentrations. Our present study focuses on n-type bulk crystals of ZnO having $n_{300 \text{ K}}$ varying from 10^{13} to 10^{18} cm^{-3}. Our sample set represents variations in PL edge emission energy of 70 meV. We establish the effects that free carriers have on the band-gap and the free-exciton absorption and emission energies and we show that different samples exhibit different FX-optical-phonon coupling in emission.

n-type CVT-grown ZnO crystals exhibit a 300 K PL emission peaking near 3.26 eV due to a superposition of FX and LO-phonon replicas of the free exciton (FX-1LO, FX-2LO), with the FX-1LO being the dominant contribution.[3–5] The spectral line shape functions for FX (assuming Gaussian form) and FX-1LO are given below.[6]

FX:
$$F(E) \sim [\exp(-(E-E_x)^2/2\sigma^2)][\exp(E-E_x)/k_BT],$$
(1)

FX-1LO:
$$F(\varepsilon) \sim \varepsilon^{1/2}[\exp(-\varepsilon/k_BT)]W(\varepsilon).$$
(2)

Here, ε is $E - E_x - \hbar\omega_{LO}$ and the free-exciton transition energy E_x is $E_g - 60$ meV. $W(\varepsilon)$ is the transition probability for the phonon-assisted transition and varies as ε^p, where the parameter p is between 0 and 1. From Eq. (1), the FX peak energy is lower than the E_x transition energy by an amount $\sigma^2/k_BT = (\text{FWHM})^2/(k_BT8 \ln 2)$. If the full width at half maximum (FWHM) varies as k_BT, then the energy offset σ^2/k_BT at 300 K is ~ 5 meV. From Eq. (2), the FX-1LO emission peaks at an energy that is higher than $E_x - \hbar\omega_{LO}$ by an amount $(p + \frac{1}{2})k_BT$. With an $\hbar\omega_{LO}$ of 72 meV and $p = 1$, the FX-1LO emission peak in ZnO at 300 K will be 33 meV lower than E_x.

Eleven bulk ZnO c-plate crystals, representing three growth methods, were used in our study. Six samples were grown by the hydrothermal technique: A (Airtron, NJ), B and C (Tokyo Denpa, Japan), D and E (Hanscom AFB, NY), and F (MTI). Three samples (G–I) were grown by the seeded CVT method (Eagle-Picher, OH), and two were grown by a high-pressure process (Cermet, GA). Sample I has been annealed in zinc vapor,[7] and sample G is as grown but contains a large amount of nitrogen acceptors (electron paramagnetic resonance (EPR) and PL have been reported[8–10] for samples from this boule). Hall measurements were made using a van der Pauw geometry. The 325 nm output of a He–Cd laser was used (incident power density was ~ 0.5 W/cm^2). PL was detected using a 0.64 m monochromator and a GaAs photomultiplier tube with photon-counting electronics. Data were corrected for the system response.

[a] Electronic mail: nancy.giles@mail.wvu.edu
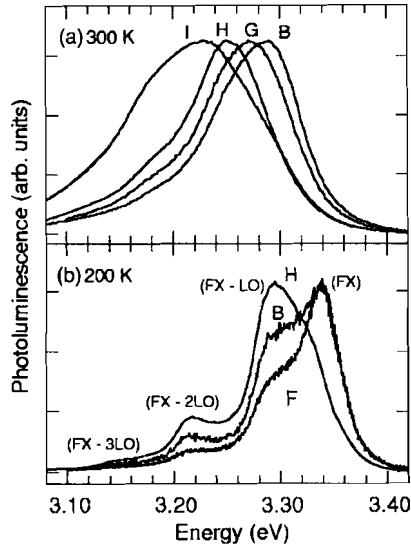[b] Also at Solid State Scientific Corporation, 27-2 Wright Road, Hollis, NH 03049.

FIG. 1. (a) PL spectra taken at 300 K for ZnO samples B, G, H, and I. (b) PL spectra taken at 200 K for ZnO samples B, F, and H. The FX and FX-nLO emissions are labeled.

FIG. 2. (a) Predicted magnitudes of energy shifts due to E_F, E_c^c, and E_c^e in n-type ZnO, from Eqs. (3)–(5). (b) Decrease in energy gap with and without band filling for $\alpha=0$ (solid curves) and $\alpha=0.502$ (dashed curves).

Figure 1(a) shows room-temperature PL emission from four samples. The intensities have been normalized to allow easier comparison of the peak positions. The temperature dependence of the near-edge emission from several samples revealed that the superposition of FX and FX-1LO bands at higher temperatures were similar to that reported in Refs. 3–5; however, the relative intensities of the FX to FX-1LO emission were not constant among the samples. Figure 1(b) shows PL taken at 200 K from three samples (intensities have been normalized). The FX-nLO emissions ($n=1,2,3$) can still be resolved at 200 K, and it is clear that the FX to FX-1LO intensity ratio is much higher for samples B and F. In the remainder of this letter, we present a model to explain shifts in E_x as a function of carrier concentration. Once those energy shifts are included, the remaining variations in PL peak position are proposed to be a direct result of different relative exciton-optical-phonon scattering strengths.

Analysis of near-band-edge PL from heavily doped n-type semiconductors involves band filling, band-gap shrinkage, and band tailing. In general, (e,h) recombination is described by $E_{e,h}=E_{g,0}+E_F^*-E_c^{c^*}-E_c^e$, where $E_{g,0}$ is the unperturbed band gap in the limit of no carriers, E_F^* is the Fermi energy corrected for nonparabolicity, $E_c^{c^*}$ is the band tailing due to the electron-impurity interaction for screened Coulomb potentials and nonparabolic bands, and E_c^e is the band-gap shrinkage due to the exchange interaction between free carriers.[11–13]

$$E_F^*=E_F^0\left(1-\alpha\frac{E_F^0}{E_g}\right),\qquad E_F^0=\left(\frac{\hbar^2}{2m^*}\right)(3\pi^2 n)^{2/3},\qquad (3)$$

$$E_c^{c^*}=E_c^c\left(1-2\alpha\frac{E_F^0}{E_g}\right),\qquad E_c^c=\left(\frac{\pi^{4/3}\hbar^2}{3^{1/3}}\right)\left(\frac{1}{m^*}\right)n^{2/3},\qquad (4)$$

$$E_c^e=(e/2\pi\varepsilon_r\varepsilon_0)(3/\pi)^{1/3}n^{1/3}.\qquad (5)$$

Here, E_F^0 is the Fermi energy, E_c^c is the Coulomb energy for parabolic bands, and α is a dimensionless nonparabolicity coefficient. Taking the conduction band polaron effective mass to be $m^*=0.29m_0$ and the relative static dielectric con-
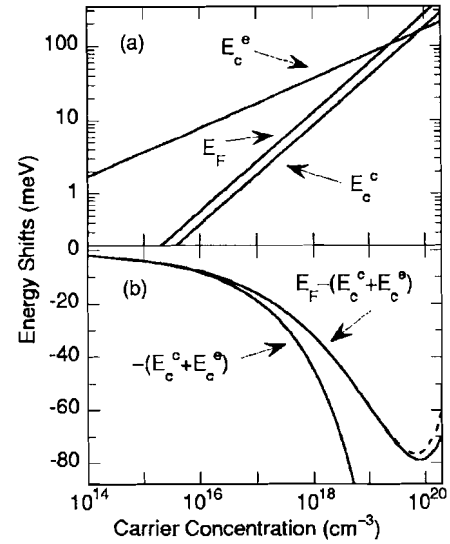
stant to be $\varepsilon_r=7.8$, the expressions (in eV) for E_F^0, E_c^c, and E_c^e become $E_F^0=1.26\times 10^{-14}n^{2/3}$, $E_c^c=8.39\times 10^{-15}n^{2/3}$, and $E_c^e=3.64\times 10^{-8}n^{1/3}$ where n has units of cm^{-3}. Ignoring crystal-field splitting[11,12] gives $\alpha=0.504$. Including crystal-field splitting[13] ($\Delta_{cf}=0.0417$ eV in ZnO) gives $\alpha=0.502$. Exciton energies are influenced by band-gap shrinkage and band tailing (the exchange and Coulomb interactions), but not band filling. Thus, the free-exciton transition energy is $E_x=E_{x,0}-(E_c^c+E_c^e)$, where $E_{x,0}$ is the transition energy in the limit of no carriers.

The predicted magnitudes of the band filling (E_F^0), Coulomb (E_c^c), and exchange (E_c^e) effects in ZnO are plotted versus carrier concentration in Fig. 2(a). Nonparabolicity effects are negligible up to mid-10^{19} cm^{-3} because of the large E_g of ZnO. (Reference 14 for ZnO:Ga films showed measurable changes due to nonparabolicity for $n>10^{16}$ cm^{-3}.) Energy shifts are very small for $n_{300\,K}<10^{15}$ cm^{-3}, so low n-type ZnO samples, e.g., compensated crystals grown by the hydrothermal method, have exciton transition energies that are closer to "perfect" ZnO. In Fig. 2(b), the net change in the optical gap, given by $E_F^*-(E_c^c+E_c^e)$, and the net change in exciton energies, $-(E_c^c+E_c^e)$, are shown (solid curves use $\alpha=0$ and dashed curves use $\alpha=0.502$). Since nonparabolicity becomes important only for $n>10^{19}$ cm^{-3}, the two curves for $-(E_c^c+E_c^e)$ and $-(E_c^{c^*}+E_c^e)$ are indistinguishable over the range shown. The optical band gap first decreases slightly, and then increases for $n\geqslant$ mid-10^{19} cm^{-3}. A "bowing" in energy gap was also predicted in a treatment[15] of heavily doped ZnO:Al films having $n\geqslant 10^{20}$ cm^{-3} (for n exceeding the Mott density, nonexcitonic recombinations are expected and the analysis of PL will differ from this present discussion).

Figure 3 shows the 300 K PL peak energies from our ZnO samples as a function of $n_{300\,K}$. The top curve is the predicted concentration-dependent E_x transition energy, the next curve is the predicted FX emission peak using the 5 meV offset, and the bottom curve is the predicted FX-1LO peak (assuming $p=1$). Equations (4) and (5) give energy shifts, so the vertical positions of the curves in Fig. 3 are adjusted to agree with the experimental results from Refs. 3–5 for the FX-1LO emission. The room-temperature
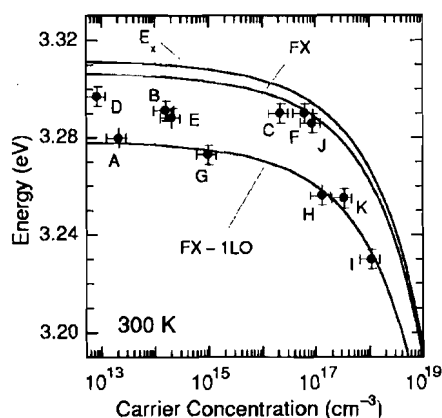
FIG. 3. PL peak energies at 300 K vs carrier concentration for 11 ZnO samples. The solid curves are the calculated dependences of E_x, FX, and FX-1LO energies on carrier concentration at 300 K in n-type ZnO.

free-exciton energy in ZnO, extrapolated to a dilute carrier concentration, is then $E_{x,0} = 3.312$ eV (± 4 meV). We ignored the effects of the small polariton splitting ($\sim 1-2$ meV) in establishing the E_x and FX energies. Using a 60 meV exciton binding energy, this results in a band gap of $E_{g,0} = 3.372$ eV for ZnO.

Five of the data points fall on or near the FX-1LO curve in Fig. 3. Three of those four samples were grown by the CVT method, and thus do not contain large concentrations of lithium or deep donors. Differences in $n_{300\,K}$ among these three samples are due to different relative concentrations of shallow donors and shallow (i.e., nitrogen) acceptors; no significant presence of other impurities was found for these samples using EPR. Sample K is melt grown, and EPR showed only a large concentration of shallow donors. Sample A was grown ~ 20 years ago by the hydrothermal technique and EPR showed that it contained much fewer transition-metal ions than the other present-day commercial hydrothermal crystals used in this study (samples B–F had much larger EPR signals from substitutional Mn^{2+}, Fe^{3+}, Ni^{3+}, and Co^{2+}). The other six ZnO samples are hydrothermal or high-pressure melt grown and these have PL peak energies between the FX-1LO and FX curves in Fig. 3. Sample F, which has dominant FX emission at 200 K [see Fig. 1(b)], also shows the weak phonon coupling at room temperature.

A significant variation in FX-phonon coupling exists among these ZnO samples. This variation is due to different exciton annihilation processes, i.e., excitons can be scattered by lattice defects (including impurities) or by phonons. Exciton scattering by LO phonons is a particularly efficient luminescence path,[16] and samples A, G, H, I, and K exhibit the lower PL peak energy as a result of this process. For most hydrothermally grown ZnO samples, which contain large concentrations of neutral and ionized impurities, the limiting factor to the exciton lifetime will be impurity scattering. Sample-to-sample variations in concentrations of lattice defects and impurities will then result in different relative strengths of the FX and FX-1LO emissions. Scattering mechanisms affecting electron mobilities in n-type ZnO also support this model. The room-temperature intrinsic mobility is limited by optical-phonon scattering. However, neutral and ionized impurity scattering is important in compensated crystals containing high concentrations of impurities of lattice defects. In samples like the CVT-grown crystals where

optical-phonon scattering is the dominant 300 K mobility-limiting factor, the PL peak will correspond to the FX-1LO energy. In samples where impurity scattering is dominant, the PL peak will lie between FX-1LO and FX. Thus, defect-associated recombination paths (donor-hole, donor-acceptor, bound exciton, etc.) do not directly contribute to the 300 K PL emission from these n-type ZnO crystals; however, defects do play a role in determining the relative strengths of FX to FX-1LO emission intensities. Also, variations in free-carrier concentration over the sample volume being probed will produce larger PL linewidths for $n > 10^{18}$ cm^{-3} (e.g., sample I) as a result of the marked increase in the slopes of the FX and FX-1LO curves.

We can extend our analysis and briefly consider higher doping levels where exciton formation may be suppressed and (e,h) or (D,h) may be present, as suggested for ZnO:Ga films.[17] A blueshift in the near-edge PL energy of ~ 0.1 eV was reported in Ref. 17 for doping concentrations up to 6×10^{20} cm^{-3}. The blueshift in (e,h) recombination, predicted using our approach, is also about 0.1 eV if n varies from 1×10^{20} to 6×10^{20} cm^{-3}.

[1]D. C. Look, D. C. Reynolds, J. R. Sizelove, R. L. Jones, C. W. Litton, G. Cantwell, and W. C. Harsch, Solid State Commun. **105**, 399 (1998); D. C. Look, B. Claflin, Ya. I. Alivov, and S. J. Park, Phys. Status Solidi A **201**, 2203 (2004).

[2]K. Maeda, M. Sato, I. Niikura, and Tsuguo Fukuda, Semicond. Sci. Technol. **20**, S49 (2005).

[3]Lijun Wang and N. C. Giles, J. Appl. Phys. **94**, 973 (2003).

[4]D. W. Hamby, D. A. Lucca, M. J. Klopfstein, and G. Cantwell, J. Appl. Phys. **93**, 3214 (2003).

[5]W. Shan, W. Walukiewicz, J. W. Ager III, K. M. Yu, H. B. Yuan, H. P. Xin, G. Cantwell, and J. J. Song, Appl. Phys. Lett. **86**, 191911 (2005).

[6]H. Barry Bebb and E. W. Williams, in *Semiconductors and Semimetals*, edited by R. K. Willardson and A. C. Beer (Academic, New York, 1972), Vol. 8, pp. 289–295 (in the figure on p. 291 and in the text on p. 295, the value of 2/3 should be 3/2).

[7]L. E. Halliburton, N. C. Giles, N. Y. Garces, Ming Luo, Chunchuan Xu, Lihua Bai, and L. A. Boatner, Appl. Phys. Lett. **87**, 172108 (2005).

[8]N. Y. Garces, Lijun Wang, N. C. Giles, L. E. Halliburton, G. Cantwell, and D. B. Eason, J. Appl. Phys. **94**, 519 (2003).

[9]Lijun Wang and N. C. Giles, Appl. Phys. Lett. **84**, 3049 (2004).

[10]Lijun Wang, N. Y. Garces, L. E. Halliburton, and N. C. Giles, Mater. Res. Soc. Symp. Proc. **799**, 261 (2004).

[11]M. Bugajski and W. Lewandowski, J. Appl. Phys. **57**, 526 (1985).

[12]I. T. Yoon, T. S. Ji, S. J. Oh, J. C. Choi, and H. L. J. Park, J. Appl. Phys. **82**, 4024 (1997).

[13]Lihua Bai, Chunchuan Xu, K. Nagashio, Chunhui Yang, R. S. Feigelson, P. G. Schunemann, and N. C. Giles, J. Phys.: Condens. Matter **17**, 5687 (2005).

[14]J. D. Ye, S. L. Gu, S. M. Zhu, S. M. Liu, Y. D. Zheng, R. Zhang, and Y. Shi, Appl. Phys. Lett. **86**, 192111 (2005). Their band-gap renormalization (varying as $n^{1/3}$) was a fitting result and a value for the nonparabolicity constant "C" in their Eq. (4) was not specified.

[15]B. E. Sernelius, K.-F. Berggren, Z.-C. Jin, I. Hamberg, and C. G. Granqvist, Phys. Rev. B **37**, 10244 (1988).

[16]C. Klingshirn, *Semiconductor Optics*, 2nd ed. (Springer, Berlin, 2005), pp. 306–312.

[17]T. Makino, Y. Segawa, S. Yoshida, A. Tsukazaki, A. Ohtomo, and M. Kawasaki, Appl. Phys. Lett. **85**, 759 (2004).